

# On-Device Neural Net Inference with Mobile GPUs

Juhyun Lee, Nikolay Chirkov, Ekaterina Ignasheva, Yury Pisarchyk, Mogan Shieh,  
Fabio Riccardi, Raman Sarokin, Andrei Kulik, and Matthias Grundmann

Google Research

1600 Amphitheatre Pkwy, Mountain View, CA 94043, USA

{impjdi, chirkov, eignasheva, ypisarchyk, moganshieh, fricc, sorokin, akulik, grundman}@google.com

## Abstract

*On-device inference of machine learning models for mobile phones is desirable due to its lower latency and increased privacy. Running such a compute-intensive task solely on the mobile CPU, however, can be difficult due to limited computing power, thermal constraints, and energy consumption. App developers and researchers have begun exploiting hardware accelerators to overcome these challenges. Recently, device manufacturers are adding neural processing units into high-end phones for on-device inference, but these account for only a small fraction of handheld devices. In this paper, we present how we leverage the mobile GPU, a ubiquitous hardware accelerator on virtually every phone, to run inference of deep neural networks in real-time for both Android and iOS devices. By describing our architecture, we also discuss how to design networks that are mobile GPU-friendly. Our state-of-the-art mobile GPU inference engine is integrated into the open-source project TensorFlow Lite and publicly available at <https://tensorflow.org/lite>.*

## 1. Introduction

On-device machine learning (ML) offers a variety of benefits. The most apparent is the improved inference latency: By skipping the data upload to the server and wait-time for the inference result, the app can respond more quickly to the user’s request. Removing the server dependency has additional benefits, such as:

- Removing the need to maintain inference servers,
- Running with limited or no connectivity, and
- Reducing privacy concerns as the user data remains on the device.

However, on-device ML is not trivial. Despite both recent advances in mobile hardware technology and efforts to efficiently run deep networks on mobile devices, mobile CPUs continue to be less powerful than those found

in servers. Running deep net inference on a mobile device means adding a significant compute-intensive task to the CPU which competes with existing logic. Fully utilizing the mobile CPU comes with additional unwanted costs, e.g. increased energy consumption leads to shorter battery life and an increase in the phone’s thermal profile causes throttling resulting in slower computation.

Hardware accelerators such as the digital signal processors offer solutions to overcome these challenges. The demand for on-device ML has led to recent trends of phone manufacturers integrating dedicated neural processing units (NPUs) for high-end next-generation phones, which account for only a small fraction of the current distribution of mobile devices.

Our primary goal is a fast inference engine with wide coverage for TensorFlow Lite (TFLite) [8]. By leveraging the mobile GPU, a ubiquitous hardware accelerator on virtually every phone, we can achieve real-time performance for various deep network models. Table 1 demonstrates that GPU has significantly more compute power than CPU.

Device	CPU (FP32)	GPU (FP16)
Samsung Galaxy S5	79	300
Samsung Galaxy S7	124	730
Samsung Galaxy S9	270	730

Table 1. Example of available compute power on mobile in gigaflops (billion floating point instructions per second). FP16 and FP32 refer to 16- and 32-bit floating point arithmetic, respectively.

This paper presents the techniques we adopt for TFLite GPU and how we achieve an average acceleration of 2–9× for various deep networks on GPU compared to CPU inference. We first describe the general mobile GPU architecture and GPU programming, followed by how we materialize this with Compute Shaders for Android devices, with OpenGL ES 3.1+ [16] and Metal Shaders for iOS devices with iOS 9+ [1].

## 2. Related Work

Various research efforts from both academia and industry endeavor to bring deep neural networks inference previously limited to server, forward to mobile devices. Those efforts can be roughly categorized into three strategies:

- Network architecture-driven,
- Hardware-driven, and
- ML framework-driven.

Neural network researchers have focused on optimizing their network architectures explicitly for processing on-device in various domains such as image classification [10, 21], object localization [11], and image enhancements [13, 14]. Many of these techniques involve reducing the model size by re-designing the network architecture and adding pre-/post-training quantization of weights. With these, one can achieve faster computation and smaller memory footprint, leading to reduced inference latency at the cost of slightly degraded model accuracy. MorphNet [9] takes a unique path of reducing the number of floating point operations per second which is optimized during training of the model. Our work is complementary to these efforts and instead focuses on optimizing the inference engine that runs the neural network rather than the model or training.

Major hardware manufacturers have made architectural changes responding to demands for faster mobile inference, and are publishing software development kits (SDKs) to expose those: Arm Compute Library [4], Huawei HiAI SDK [12], MediaTek NeuroPilot SDK [17], and Qualcomm SNPE SDK [20]. These libraries are vendor-specific and either cannot be re-used on a different architecture or do not guarantee the expected performance boost on other platforms. Our work does not add new hardware or SDKs. Instead, we use well-established hardware, the mobile GPU, and well-supported graphics and compute standards as OpenGL [16] and Metal [1], to achieve high-performance neural network inference.

Apple presented the Metal Performance Shaders with support of convolutional neural networks [3] accelerated by GPU. This is a solution built on top of the Metal API and allows custom operations. Our approach is analogous to Apple’s on iOS devices. Apple also released CoreML [2], an end-to-end solution for inference on mobile devices using CPU, GPU, and NPU, if available.

Android introduced the Android Neural Networks API [7] that serves as a layer between hardware and higher-level ML frameworks that vendors must implement for Android 8.1 or later. Our work has wider coverage and does not depend on a specific Android version, or require vendors to implement individual APIs for deep network processing.

Some of the latest mobile-friendly ML frameworks are:

- Caffe2 [6] which focuses on CPU inference and uses Arm Compute Library for Arm Mali GPUs.

- MACE [24] which employs OpenCL which is not a part of standard Android OS.

TFLite GPU leverages the mobile GPU with OpenGL ES for Android devices and Metal for iOS devices. The specific version requirements are OpenGL ES 3.1+ and iOS 9+ which are available for more than 52% of all Android devices [23]. One of our biggest strength is that our framework employs open standards, *i.e.* is not limited by specific hardware vendor, and thus covers a wide range of devices.

## 3. General Architecture

This section explains the general architecture of TFLite GPU, consisting of an initialization phase followed by a model inference phase. The techniques in this section are independent of the architecture of the underlying GPU.

### 3.1. Initialization

TFLite provides APIs for the delegation of the execution of neural network sub-graphs to another library. We exploit this feature to integrate the GPU backend into TFLite. Given a neural net model, TFLite first checks whether it can execute all the operators in the model with our GPU delegate. Our GPU backend identifies supported operators, and TFLite then partitions the graph into several sub-graphs, substituting the sub-graphs with virtual “delegate nodes”. From that point, the GPU backend is responsible for executing this sub-graph, as depicted in Figure 1. Unsupported operators are by default computed by the CPU. Ideally, the whole graph would be compatible with our mobile GPU backend for maximum performance.

As our mobile GPU inference engine is primarily designed for high-performance execution, we first inspect the model and resolve obvious inefficiencies. For example:

- Merging PAD as an option of another op where it was previously described separately.
- Removing superfluous identity operations, *e.g.* RESIZE with scale one or single input ADD/CONCAT.

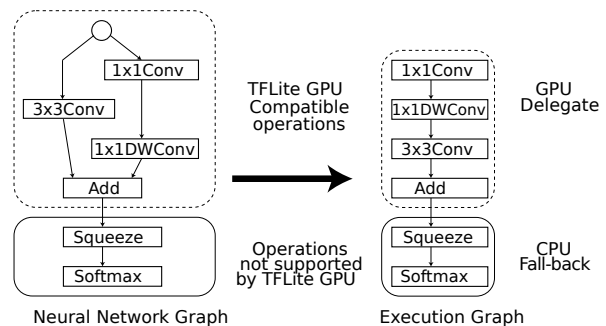


Figure 1. TFLite’s delegate mechanism: Operations supported by the GPU delegate will run on the GPU, and the rest on the CPU.

While these inefficiencies might be caught by the architect, artifacts such as these crop up inevitably, and we should still optimize these whenever possible.

Note that, in contrast to CPU backends which work without initialization, GPU backends require initialization involving shader compilation and optimization by the driver before inference. The cost of this process depends on network size and may take from few milliseconds to seconds, but is incurred once and not again for subsequent runs until the cache memory is invalidated for any of reasons: application is updated or re-installed, device is rebooted, cache memory is over, or for other OS-specific reasons.

### 3.2. Running Inference

The inference phase is fairly straightforward. The input tensors are reshaped to the PHWC4 format detailed later in Section 4, if their tensor shape has channel size not equal to 4. For each operator, shader programs are linked by binding resources such the operator’s input/output tensors, weights, *etc.* and dispatched, *i.e.* inserted into the command queue. The GPU driver then takes care of scheduling and executing all shader programs in the queue, and makes the result available to the CPU by the CPU/GPU synchronization. There might be a final conversion from PHWC4 to HWC, if the output tensor has a channel size not equal to 4.

For maximum performance, one should avoid CPU/GPU synchronization at all cost, and preferably, never leave GPU context if real-time processing is needed. The most ideal scenario would be the following: A camera provides with RGBA texture that goes directly to TFLite GPU and the output of the network is then directly rendered to the screen.

**Shader Program Optimization** In the GPU inference engine, operators exist in the form of shader programs. The shader programs eventually get compiled and inserted into the command queue and the GPU executes programs from this queue without synchronization with the CPU.

To reduce the number of shader programs in the command queue, we consolidate them into meaningful aggregates while maximizing parallelism and well-defined data dependencies. The following techniques are employed when generating the source code for the shader programs:

- Fusing element-wise operators with computationally expensive operators, *e.g.* activations with convolution, to reduce the number of shader programs.
- In-lining parameters and small objects directly into the shader program to reduce memory I/O overhead.
- Baking uniforms into the source code, instead of passing them in the run-time, allowing drivers to produce more optimal code.
- Creating specialized version of shaders, like “convolution with  $1 \times 1$  kernel size”, to manually optimize shaders for particular cases.

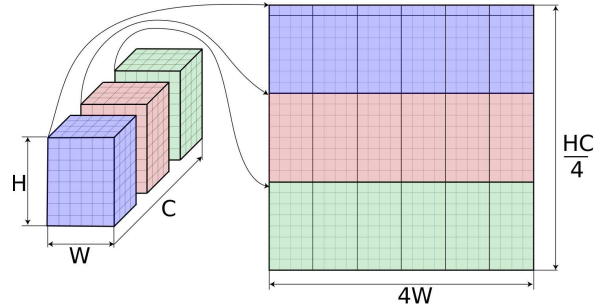


Figure 2. Example of PHWC4 memory layout (best viewed in color). A tensor of shape  $(H=8, W=6, C=12)$  is split into 4-element slices of size  $(H, W, 4)$  which are stored sequentially as a continuous 2D array of size  $(HC/4=24, 4W=24)$ .

- Implementing specialization of shader programs optimized for a certain architecture to improve the op’s performance on the said environment.

After the source code for each program is generated, each shader gets compiled. This compilation step can take a while, from several milliseconds to seconds. Typically, app developers can hide this latency while loading the model or starting the app for the first time. Once all shader programs are compiled, the GPU backend is ready for inference.

## 4. Data Layout

Most modern GPUs use a homogeneous coordinate [18] system which represents points in space with coordinates  $(x, y, z, w)$ . A homogeneous coordinate  $(x, y, z, w)$ , where  $w \neq 0$ , represents a point  $(x/w, y/w, z/w, 1)$  in a 3D space. This allows affine transformations and projective transformations to be represented in the form of 4D matrix multiplications. GPUs are essentially processors optimized for 4-element vector compute and load/store operations.

While TFLite does not restrict tensors to a certain shape, many operators assume 4D input/output tensors shaped as  $[B, H, W, C]$  where  $B, H, W, C$  respectively represent batch size, height, width, and channel size. For convenience, the rest of the paper will mostly describe tensors assuming a batch size of 1, or  $[H, W, C]$  for short. This simplified example can be generalized if we consider batches to be a concatenation of multiple  $[H, W, C]$  tensors.

In TFLite GPU, a  $[H, W, C]$  tensor is split into 4-channel slices which are stored sequentially in memory. If the number of channels is not divisible by 4, it is padded with zeroes. This memory layout, called PHWC4 (Figure 2), optimally reduces cache misses in the graphics architecture. This is tightly coupled with how compute threads are executed on the GPU, which defines the order of computation, and more importantly, the order of memory load instructions.

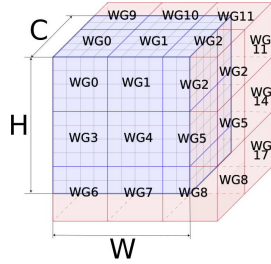


Figure 3. Compute shader execution grid ( $X=12, Y=12, Z=8$ ) built upon the tensor shape ( $H=10, W=10, C=6$ ) shown in blue (best viewed in color). Work group size ( $x=4, y=4, z=4$ ) highlighted as cubes with bold lines. Each cell represents a FP32 value.

#### 4.1. Work Groups: GPU Threading Units

A GPU compute task consist of a shader program and a grid. Every thread executes the same shader program, but on different region of a 3D mesh problem space. The global grid is made up of repeated work groups of constant shape  $(x, y, z)$  and has a total dimension  $(X, Y, Z)$  which is a multiple of these work groups.

Every operation in the graph has at least one output 3D tensor. If there is more than one output tensor, we use one of them as a basis for the compute grid size calculation. The grid may be larger than the actual output tensor, because we expand it to sizes in multiples of 4 due to GPUs working efficiently for those sizes. This causes the creation of threads which do nothing and return at the beginning of the main function, but this is faster than working with misaligned grid sizes which prevents efficient optimization of byte code. The described situation is visualized in Figure 3, where blue color highlights useful threads which will actually calculate output values, and red color highlights stub threads. Further tuning of the compute grid/work group sizes is described in subsection 4.2.

Optimizations are focused on neighboring threads *within* a work group - those spawned in sequential order as described. The PHWC4 layout provides the advantage of allowing neighboring threads to hit the same cache line when requesting data for input tensors.

Threads inside a work group are executed in a particular order. Our experiments show that for each work group channel, each row is sequentially picked in order from the first to last, starting across  $W$ , then  $H$  and finally  $C$ . Ordering of work group execution is likewise sequential and follows the same schema, as shown on Figure 3.

**For a 2D Convolution,** we compute the result at every output element, by iterating over the weights of a convolution kernel and its corresponding input elements covered by a window of size  $(kernel\_height, kernel\_width)$ . For simplicity, we consider the case of  $1 \times 1$  convolution window case. In this case, only one input cell is needed to calculate

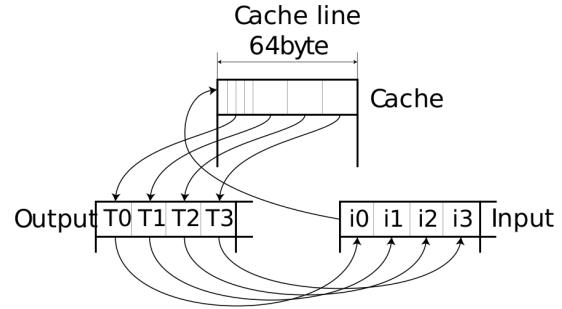


Figure 4. Cache hit by 4 neighboring threads. When threads  $T_0-T_3$  each issue a 16-byte load of memory blocks  $i_0-i_3$  that are contiguous in memory, the first load can fill the 64-byte cache line, benefiting the other threads with no additional cost in memory I/O.

one output element. As we work with 3D tensors, every cell is implied to be a vector of channels. For this operation, every thread at the very first iteration of its loop requests first 4 channels of the appropriate cell. A compulsory cache miss occurs on the initial thread request (for 16 bytes, or 4 float values), which triggers the actual data load. When this occurs, the hardware memory manager loads the whole cache line and not just the requested 16 bytes. Since the cache line size on most mobile GPUs is 64 bytes, this results in the loading of the next 48 bytes as well. Since all threads execute the same shader code, the neighboring threads will also execute the same code as the first one (the initially requested 16 bytes). Organizing threads in the way is an efficient strategy for memory loading as the next (neighboring) input values will already be available when requested and loaded as part of the same cache line for initial neighbor compute threads (Figure 4).

#### 4.2. Work Group Size Selection

The work group size for executing shader programs defines the group of threads which share data inside the work group. Depending on the GPU, picking the right work group size can result in increased performance, whereby picking the wrong can result in unexpected slowdowns. Arm Mali GPUs, for instance, show robust performance independent of configured work group sizes and tuning them only results in a nominal performance gain typically less than 5%. Qualcomm Adreno GPUs, on the other hand, are extremely sensitive to well-configured work group sizes and tuning these can give up to a 30% performance boost.

Tuning the work group size is unfortunately difficult as GPU internals are not available to the user either directly (via the API), or indirectly (via some assembly representation of internal state). Threads are executed in groups called “waves” and knowing the wave size is crucial to optimizing the work group size as they fine-tune the memory usage of neighboring threads. Devising an algorithmic selection of



optimal work group size thus becomes an exhaustive search. Note that selecting the wrong work group size may slow down execution by 5–7 times on Adreno GPUs.

Despite these challenges, we conducted extensive investigations into optimizing the work group size, focusing primarily on CONV\_2D and DEPTHWISE\_CONV, as these make up nearly 90% of the workload for convolutional networks. While the algorithmic solution is not perfect, the alternative brute-force approach is impractical for real time applications because the work group investigation for a model may take several minutes. In addition, measurements may be inconsistent due to device temperature, resource racing, etc., causing the true global optimal work group size to change from one inference to another.

Because of these fluctuations, we approximate a reasonable optimum within the neighborhood region of the global optimum given an inference time function  $T(W, C)$ , where  $W$  is work group sizes, and  $C$  identifies convolution configuration. The domain of the function parameters are:

- Work groups dimensions  $W$ : 2, 4, or 8
- Convolution configurations  $C$  search space:
  - CONV\_2D weights  $1 \times 1, 2 \times 2, 3 \times 3$ , or
  - DEPTHWISE\_CONV input and output shapes from  $(8, 8, 8)$  to  $(128, 128, 128)$ , and
  - Strides  $1 \times 1, 2 \times 2, 3 \times 3$

Given the search space defined by the convolution configuration, a gradient descent approach allows us to converge on a stable optimum work groups where expected performance varies 10% on every inference. From this region of stable work groups, an approximate optimal work group can be selected for every device and convolution type combination.

Work groups from the Table 2 are currently used in TFLite GPU and their stability is statistically proven. While they do not necessarily result in peak optimal time across all parameters, they are reliable in giving top 10% performance regardless of the convolution parameters.

Adreno GPU Model	CONV_2D	DEPTHWISE_CONV
630	(4, 8, 4)	(4, 4, 8)
540	(8, 2, 2)	(8, 8, 2)
510	(8, 4, 4)	(8, 4, 4)
509	(8, 4, 8)	(8, 4, 2)
50X/4XX	(8, 4, 8)	(8, 4, 8)

Table 2. Optimal work group sizes for Adreno GPUs.

## 5. Memory Manager for Intermediate Tensors

While we allocate GPU memory for all input/output tensors and tensors holding the trained weights, we do not allocate memory for all intermediate tensors between the operators separately, as they do not have to co-exist in memory

simultaneously. This is an important optimization to reduce the memory footprint of the GPU run-time.

During initialization, we first topologically sort the network to determine the execution order of each operator, and the correspondingly required tensors. For each intermediate tensor, we can determine the first and the last operator that uses this tensor either as input or output. Once the last “consumer” of an intermediate tensor has finished executing, the memory for the said intermediate tensor can be re-used for other intermediate tensors. To minimize the total required memory allocation, we have devised a strategy to determine when this final operator execution has occurred. This problem is NP-complete [22].

We compared three algorithms for managing the intermediate tensors: (a) a naïve algorithm, (b) a greedy algorithm, and (c) a minimum-cost flow algorithm. The first just naïvely allocates all memory necessary and only serves as a baseline for comparison. The latter two implement smart memory management and use the concept of “shared objects” by which we refer to as allocated memory that is used for more than one tensor during inference, but not more than exactly one at a time. The size of the shared object is the maximum of sizes of tensors that it is used for. For example, if a shared object  $S$  is used for tensor  $a$ , re-used for tensor  $b$ , and later for tensor  $c$ , the size of the shared object  $S$  needs to be  $size_S = \max(size_a, size_b, size_c)$ .

**The Greedy Algorithm** is summarized in Algorithm 1. We iterate through all operators in topological execution order. If an output tensor of the current operator is an intermediate tensor, it is assigned to a newly created shared object

---

### Algorithm 1 Greedy Memory Management

---

```

1: available_objects  $\leftarrow \emptyset$ 
2: used_objects  $\leftarrow \emptyset$ 
3: for each  $op \in operators$  do
4:   for each  $t \in op.outputs$  do
5:     if  $t$  is intermediate then
6:       if available_objects =  $\emptyset$  then
7:          $S \leftarrow$  new shared object with size  $t.size$ 
8:       else
9:          $S \leftarrow available\_objects.find(t.size)$ 
10:        available_objects.remove( $S$ )
11:        if  $t.size > S.size$  then
12:           $S.size \leftarrow t.size$ 
13:         $t.shared\_object \leftarrow S$ 
14:        used_objects.insert( $S$ )
15:   for each  $t \in op.inputs$  do
16:     if  $t$  is intermediate and  $op$  is its last consumer then
17:        $S \leftarrow t.shared\_object$ 
18:       used_objects.remove( $S$ )
19:       available_objects.insert( $S$ )

```

---

if the pool of shared objects is empty (L.7), or to an existing shared object that has the closest size by absolute difference to the  $t.size$  (L.9) which gets removed from the available pool (L.10). If  $t.size > S.size$ , then the shared object's buffer size is increased (L.11–12). This shared object  $S$  is inserted into the set of currently used objects (L.14). After the output tensors, the input tensors are inspected. If an input tensor is an intermediate tensor and the current operator is the last consumer, we remove the shared object that is assigned to this tensor from the set of currently used objects, and add it back to the pool of shared objects (L.17–19).

This algorithm has the runtime complexity of  $O(n \log n)$  where  $n$  is the number of intermediate tensors. We use binary search tree for the pool of shared objects and binary heap priority queue for the set of currently used objects. Straightforward implementation of the same algorithm without these data structures has a run-time complexity of  $O(n^2)$ . For the neural network from Figure 5, this approach re-uses memory of output tensor of vertex 0 for output tensor of vertex 2, and memory of output tensor of vertex 1 for output tensor of vertex 4. The total size of allocated memory is 104.

**The Minimum-Cost Flow Algorithm** involves creating an auxiliary flow network and solving the minimum-cost flow problem (MCFP) [5]. First, we insert two vertices for each intermediate tensor  $x$  and denote them  $l_x$  and  $r_x$  with two special vertices for the source  $s$  and the sink  $t$ . Then, we add directed edges to the flow network:

1. For each  $x$  in  $1..N$ , add an edge from  $s$  to  $r_x$  with capacity 1 and cost  $size_x$ . For tensor  $x$ , we can allocate new shared object of size  $size_x$ .
2. If a shared object allocated for tensor  $x$  can be re-used for tensor  $y$ , then add an edge from  $l_x$  to  $r_y$  with capacity 1 and cost  $\max(0, size_y - size_x)$ . If tensor  $y$  is greater in size than tensor  $x$ , we can re-use corresponding shared object, but we might need to allocate  $size_y - size_x$  of additional memory. This is not always the case, when the shared object can already have a size greater than  $size_x$ , but it is a good approximation.
3. For each  $x$  in  $1..N$ , add an edge from  $s$  to  $l_x$  with capacity 1 and cost 0.

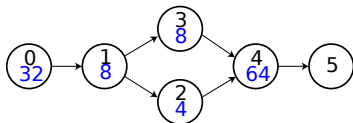


Figure 5. An example neural net. Each vertex corresponds to an op. The upper number denotes the execution order, and the lower number the size of its output intermediate tensor. The last op does not have the latter as its output is not an intermediate tensor.

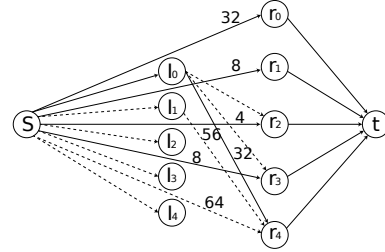


Figure 6. The flow network for the neural network in Figure 5. Capacity of each edge is 1. Saturated edges, *i.e.* the final assignment of shared objects to tensors, are shown as solid lines.

4. For each  $x$  in  $1..N$ , add an edge from  $r_x$  to  $t$  with capacity 1 and cost 0.

After building the flow network, we solve the MCFP with Shortest Path Faster Algorithm (SPFA) [19] or Johnson's algorithm [15]. With SPFA, the run-time complexity  $O(N^4)$ , but it can be reduced to  $O(N^3)$  by decreasing the number of edges of type 2. Figure 6 shows a flow network and the result of this algorithm execution for example graph from Figure 5. Minimum-cost flow approach re-uses memory of output tensor of vertex 0 for output tensor of vertex 4. The total size of allocated memory is 84.

If an edge of type 1 (from  $s$  to  $r_x$ ) is saturated by the flow, *i.e.* its residual capacity is equal to 0, we create new shared object for the tensor  $x$ . If an edge of type 2 (from  $l_x$  to  $r_y$ ) is saturated by the flow, we assign the same shared object for tensor  $y$  that was used by tensor  $x$ . After execution of the algorithm, the amount of the flow will be equal to  $N$ . It means that the resulting flow network has information about the assignment of shared objects for all  $N$  intermediate tensors. Size of each shared object is determined by the maximum size of all tensors assigned to it.

There is no clear winner between these two memory management algorithms in terms of the minimal memory footprint, and it depends on the network (Table 3). TFLite GPU is using the greedy algorithm by default with the developer being able to choose the MCFP algorithm if desired.

Strategy	MobileNet	MobileNetV2	DeeplabV3
Naïve	9.6	13.2	24.3
Greedy	<b>2.3</b>	4.0	<b>3.6</b>
MCFP	2.7	<b>3.8</b>	4.2

Table 3. Total memory allocated (in MB) for all intermediate tensors. Naïve means no memory manager and serves as baseline. Bold number means the smallest memory footprint for each model.

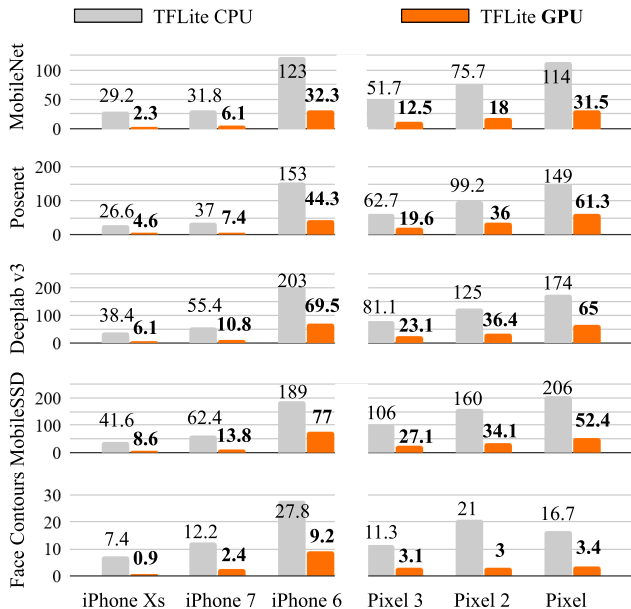


Figure 7. Average inference latency (in milliseconds) of TFLite GPU (orange) compared to CPU (gray) on various neural networks, run on a variety of smartphones (best viewed in color).

## 6. Results

Figure 7 illustrates the performance of GPU inference compared to CPU inference in TFLite for various neural networks which generally demonstrates a 2–9 $\times$  speedup. The first 10 warm-up runs were skipped for benchmarking and averages are based on the 100 subsequent inferences. This profiling revealed that TFLite GPU is often bound by memory bandwidth and we typically only see 20–40% ALU utilization. On iOS devices, we benefit from larger cache sizes that result in reduced memory I/O latency, and hence, better performance than the OpenGL backend.

Table 4 and Table 5 show the average inference latency of iOS- and Android-compatible ML frameworks on MobileNet v1, respectively. Note that TFLite GPU employs OpenGL for the widest coverage with reasonable performance. MACE and SNPE employ OpenCL and may outperform TFLite GPU on some mobile devices shipped with OpenCL. As OpenCL is not a part of the standard Android distribution, apps using those frameworks may not be able to guarantee their inference performance *e.g.* on Google Pixel devices. Also note that SNPE does not run on devices with Arm Mali GPUs.

Figure 8 shows how inference performance degrades over a sustained period of time due thermal throttling of the device. Mobile inference by applications typically occur in one of two modes: one-time detection or ongoing run-time data processing. For one-time inference, *e.g.* object detection, an application may achieve the peak perfor-

iOS Device	TFLite GPU	MPSCNN	CoreML
iPhone Xs	2.3	4.1	7.1
iPhone 7	5.5	7.9	42
iPhone 6	31	92	116

Table 4. Average inference latency (in milliseconds) of iOS-compatible ML frameworks on MobileNet v1.

Android Device	TFLite GPU	MACE	SNPE
Samsung S9 (Adreno 630)	13	12	6.9
Xiaomi Mi8 SE (Adreno 616)	35.9	29.6	20
Huawei P20 Pro (Mali G72-MP12)	13.5	45	N/A <sup>1</sup>
Google Pixel 2 (Adreno 540)	18	N/A <sup>2</sup>	N/A <sup>2</sup>
Google Pixel 3 (Adreno 630)	12.5	N/A <sup>2</sup>	N/A <sup>2</sup>

Table 5. Average inference latency (in milliseconds) of Android-compatible ML frameworks on MobileNet v1. Note that TFLite GPU employs OpenGL and thus has the widest coverage with reasonable performance. MACE and SNPE employ OpenCL and may run faster on devices shipped with OpenCL, but may not run on all devices. <sup>1</sup> Arm Mali GPUs are not compatible with SNPE. <sup>2</sup> Google Pixel devices do not support OpenCL.

mance illustrated in the left half of graph in Figure 8 where device temperature is nominal. For ongoing run-time inference, *e.g.* video segmentation, the right half illustrates the potential impact of thermal throttling due to sustained performance.

In order to avoid data transfer delays, real-time applications usually place neural network input/output tensors in a GPU texture or buffer. TFLite GPU allows using CPU-side tensors as input/output as well. Additionally, CPU-to-GPU data-transfer efficiency can be controlled via time or power efficient synchronization mechanisms. The most power-efficient one suspends waiting threads until the GPU completes its task. The fastest option by comparison, employs an active spin-lock approach, reducing data acquisition delays by avoiding operating system process re-scheduling.

## 7. Conclusion

In this paper, we presented the architectural design of TFLite GPU. We described the properties of mobile GPUs and explained optimization techniques we employed for fast memory I/O, small run-time memory footprint, and fast compute shader execution. With these, we aim to make the network architects be mobile GPU-aware when they design their networks.

From our discussion of mobile GPU-friendly data layout

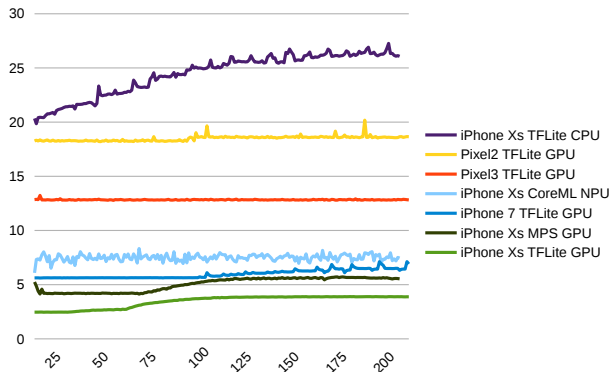


Figure 8. Inference latency (in milliseconds) for MobileNet v1 over extended period of time  $[0, 200]_{sec}$  (best viewed in color).

PHWC4, neural network designers should know that any kind of RESHAPES are significantly more expensive on the GPU than on the CPU. The network itself will learn the weights regardless of the RESHAPE op, thus it is best to skip the operator entirely if a RESHAPE operation was inserted just for convenience of the architect.

For the same reason, if the mobile device can produce RGBA rather than RGB, it is now apparent that using the former can avoid a conversion, *i.e.* memory copy, from RGBA to RGB. Similarly, if the mobile device can render a 4-channel tensor, *i.e.* RGBA, directly, that can be a better choice than the RGB counterpart. This choice benefits not just the graph input/output, but also its intermediate tensors. Similarly, since we know that a tensor of shape  $[B, H, W, 5]$ , for instance, is twice as expensive as  $[B, H, W, 4]$ , but about the same as  $[B, H, W, 8]$ , then the architect can tune around those 4-channel boundaries rather than trying to optimize on other boundaries.

TFLite GPU is still in its early development stages. We plan to investigate several areas including employing additional GPU-specific optimizations to improve inference speed further, and expanding support for more operations, *e.g.* understand more about recurring networks or LSTMs, and how we can optimize those for GPUs. Finally, we are extensively exploring other GPU backends such as OpenCL and Vulkan to achieve better ALU utilization.

## Acknowledgements

We would like to acknowledge our colleagues at TensorFlow Lite; Lawrence Chan, Tim Davis, Jared Duke, Yu-Cheng Ling, Andrew Selle, Sarah Sirajuddin, and Pete Warden. We are also grateful to Aleksandr Ignashev for the figures in this paper and Karthik Raveendran for his valuable feedback.

## References

- [1] *Metal Shading Language Specification*. Apple Inc., 2014. 1, 2
- [2] Apple Inc. Core ML. <https://developer.apple.com/documentation/coreml>. [Online; accessed Apr 8, 2019]. 2
- [3] Apple Inc. Metal Performance Shaders. <https://developer.apple.com/documentation/metalperformance-shaders>. [Online; accessed Apr 8, 2019]. 2
- [4] Arm Ltd. Compute Library. <https://developer.arm.com/ip-products/processors/malibu>. [Online; accessed Apr 8, 2019]. 2
- [5] Wikipedia contributors. Minimum-Cost Flow Problem. [https://en.wikipedia.org/w/index.php?title=Minimum-cost\\_flow\\_problem](https://en.wikipedia.org/w/index.php?title=Minimum-cost_flow_problem). [Online; accessed Apr 8, 2019]. 6
- [6] Facebook Inc. Caffe2. <https://caffe2.ai>. [Online; accessed Apr 8, 2019]. 2
- [7] Google LLC. Neural Networks API. <https://developer.android.com/ndk/guides/neuralnetwork-api>. [Online; accessed Apr 8, 2019]. 2
- [8] Google LLC. TensorFlow Lite. <https://www.tensorflow.org/lite>. [Online; accessed Apr 8, 2019]. 1
- [9] Ariel Gordon, Elad Eban, Ofir Nachum, Bo Chen, Hao Wu, Tien-Ju Yang, and Edward Choi. MorphNet: Fast & Simple Resource-Constrained Structure Learning of Deep Networks. In *IEEE Conference on Computer Vision and Pattern Recognition*, pages 1586–1595, 2018. 2
- [10] Andrew G Howard, Menglong Zhu, Bo Chen, Dmitry Kalenichenko, Weijun Wang, Tobias Weyand, Marco Andreetto, and Hartwig Adam. MobileNets: Efficient Convolutional Neural Networks for Mobile Vision Applications. *arXiv preprint arXiv:1704.04861*, 2017. 2
- [11] Jonathan Huang, Vivek Rathod, Chen Sun, Menglong Zhu, Anoop Korattikara, Alireza Fathi, Ian Fischer, Zbigniew Wojna, Yang Song, Sergio Guadarrama, and Kevin Murphy. Speed/Accuracy Trade-offs for Modern Convolutional Object Detectors. In *IEEE Conference on Computer Vision and Pattern Recognition*, pages 7310–7311, 2017. 2
- [12] Huawei Technologies Co., Ltd. HiAI Engine. <https://developer.huawei.com/consumer/en/devservice/openapi>. [Online; accessed Apr 8, 2019]. 2
- [13] Andrey Ignatov, Nikolay Kobyshev, Radu Timofte, Kenneth Vanhoey, and Luc Van Gool. DSLR-Quality Photos on Mobile Devices with Deep Convolutional Networks. In *IEEE International Conference on Computer Vision*, pages 3277–3285, 2017. 2
- [14] Andrey Ignatov, Radu Timofte, et al. PIRM Challenge on Perceptual Image Enhancement on Smartphones: Report. In *European Conference on Computer Vision*, pages 315–333. Springer, 2018. 2
- [15] Donald B. Johnson. Efficient Algorithms for Shortest Paths in Sparse Networks. *Journal of the ACM*, 24:1–13, 1977. 6
- [16] Jon Leech, editor. *OpenGL ES Version 3.1*. The Khronos Group Inc., 2016. 1, 2



- [17] MediaTek Inc. What is MediaTek NeuroPilot? <https://www.mediatek.com/blog/what-is-mediatek-neuropilot>. [Online; accessed Apr 8, 2019]. 2
- [18] August F. Möbius. *Der baryzentrische Calcul.* 1827. 3
- [19] Edward F. Moore. The Shortest Path Through a Maze. In *International Symposium on the Theory of Switching*, pages 285–292, 1959. 6
- [20] Qualcomm Inc. Snapdragon Neural Processing Engine SDK. <https://developer.qualcomm.com/docs/snpe>. [Online; accessed Apr 8, 2019]. 2
- [21] Mark Sandler, Andrew Howard, Menglong Zhu, Andrey Zhmoginov, and Liang-Chieh Chen. MobileNetV2: Inverted Residuals and Linear Bottlenecks. In *IEEE Conference on Computer Vision and Pattern Recognition*, pages 4510–4520, 2018. 2
- [22] Ravi Sethi. Complete Register Allocation Problems. *SIAM Journal on Computing*, 4:226–248, 1975. 5
- [23] Carole-Jean Wu, David Brooks, Kevin Chen, Douglas Chen, Sy Choudhury, Marat Dukhan, Kim Hazelwood, Eldad Isaac, Yangqing Jia, Bill Jia, Tommer Leyvand, Hao Lu, Yang Lu, Lin Qiao, Brandon Reagen, Joe Spisak, Fei Sun, Andrew Tulloch, Peter Vajda, Xiaodong Wang, Yanghan Wang, Bram Wasti, Yiming Wu, Ran Xian, Sungjoo Yoo, and Peizhao Zhang. Machine Learning at Facebook: Understanding Inference at the Edge. In *IEEE International Symposium on High-Performance Computer Architecture*, 2019. 2
- [24] Xiaomi. MACE. <https://github.com/XiaoMi/mace>. [Online; accessed Apr 8, 2019]. 2